740 *Chem. Mater.* **2010,** *22,* 740–742
DOI:10.1021/cm901624v

CHEMISTRY OF MATERIALS
Communication

# Using Neutron Spin−Echo To Investigate Proton Dynamics in Proton-Conducting Perovskites[†]

Maths Karlsson,*[,‡,§] Dennis Engberg,[§] Mårten E. Björketun,[§] Aleksandar Matic,[§] Göran Wahnström,[§] Per G. Sundell,[§] Pedro Berastegui,[∥] Istaq Ahmed,[⊥] Peter Falus,[#] Bela Farago,[#] Lars Börjesson,[§] and Sten Eriksson[⊥]

[‡]*European Spallation Source Scandinavia, Lund University, 221 00 Lund, Sweden,* [§]*Department of Applied Physics, Chalmers University of Technology, 412 96 Göteborg, Sweden,* [∥]*Department of Inorganic Chemistry, Arrhenius Laboratory, Stockholm University, 106 91 Stockholm, Sweden,* [⊥]*Department of Chemical and Biological Engineering, Chalmers University of Technology, 412 96 Göteborg, Sweden, and* [#]*Institut Laue-Langevin, 38042 Grenoble Cedex 9, France*

*Received June 12, 2009*
*Revised Manuscript Received October 20, 2009*

Many hydrated $ABO_3$-type perovskites are found to be fast proton conductors in the intermediate temperature range ∼200−500 °C.[1] Loading protons in the perovskite structure relies on acceptor-doping to the B site, whereby oxygen vacancies are created, which can be filled with hydroxyl groups in a humid atmosphere at elevated temperatures.[1] On a local scale the proton conduction process is composed of two elementary steps: (i) hydrogen-bond-mediated proton transfer between adjacent oxygens and (ii) rotational motion of the hydroxyl group in between such transfers.[1] The long-range motion of the protons is a series of such transfers and rotations, with an overall rate which depends on the local energy barriers.

The long-range proton diffusion constant is commonly extracted from conductivity experiments via the Nernst−Einstein relation, but there is also one example of the use of pulsed-field gradient nuclear magnetic resonance (PFG-NMR).[2] On microscopic length-scales, proton dynamics in hydrated perovskites have been investigated with frequency-resolved quasielastic neutron scattering (QENS), covering the picoseconds time-scale, extended up to ∼1 ns in some cases, in which mainly the local dynamical processes have been observed, although data have also been interpreted in terms of nonlocalized motions.[3−10] Investigations of the proton dynamics would, however, benefit greatly if one could extend the time-range to longer time-scales so that the microscopic diffusional process can be studied and information about the influence of the local structure and energy barriers on the proton diffusion can be obtained. This is indeed possible by the use of neutron spin−echo (NSE),[11−13] with which the proton dynamics can be studied over a microscopic length-scale in a wide time-range of picoseconds to microseconds. However, to our knowledge, this technique has previously not been applied to studying the proton dynamics in hydrated perovskites nor in any other proton-conducting ceramic.

In this Communication we demonstrate the applicability and potential of NSE to study proton dynamics in proton-conducting ceramics. This is exemplified by experiments performed on hydrated $BaZr_{0.90}Y_{0.10}O_{2.95}$ (10Y:BZO), a cubic perovskite with a relatively high proton conductivity.[1,14] The high proton conductivity together with a high thermodynamic stability make this material a promising candidate for use as electrolyte in intermediate temperature fuel cells.[1] In addition to our experimental work, we use kinetic modeling based on first-principles calculations to assist the interpretation of the experimental data.

The NSE experiment was performed at the IN15 spectrometer at Institut Laue-Langevin (ILL) in Grenoble, France, with which a wide time-range over nearly three decades, ∼0.2 to 50 ns, was covered. The measured quantity in NSE is the polarization of the scattered neutrons as a function of the momentum transfer $Q$ and Fourier time $t$, which is related to the intermediate scattering function $I(Q,t)$.[13] $I(Q,t)$ can be divided into a coherent and an incoherent part, which are related to the space Fourier transform of the space−time self- and pair-correlation functions, respectively, hence revealing collective and self-dynamics simultaneously.[13] As an example, for free diffusion, the incoherent $I(Q,t)$ would show an exponential relaxation, that is, $I(Q,t) = e^{-t/\tau(Q)}$, with the relaxation time $\tau$ proportional to $Q^{-2}$, namely,

[†] Accepted as part of the 2010 "Materials Chemistry of Energy Conversion Special Issue".
*Corresponding author: E-mail: maths.karlsson@esss.se.

(1) Kreuer, K. D. *Annu Rev. Mater. Res.* **2003**, *33*, 333.
(2) Kreuer, K. D.; Dippel, Th.; Baikov, Yu. M.; Maier, J. *Solid State Ionics* **1996**, *86−88*, 613.
(3) Hempelmann, R.; Karmonik, C.; Matzke, T.; Cappadonia, M.; Stimming, U.; Springer, T.; Adams, M. A. *Solid State Ionics* **1995**, *77*, 152.
(4) Matzke, T.; Stimming, U.; Karmonik, C.; Soetramo, M.; Hempelmann, R.; Güthoff, F. *Solid State Ionics* **1996**, *86−88*, 621.
(5) Gross, B.; Beck, C.; Meyer, F.; Krajewski, T.; Hempelmann, R.; Altgeld, H. *Solid State Ionics* **2001**, *145*, 325.
(6) Karlsson, M.; Matic, A.; Engberg, D.; Björketun, M. E.; Koza, M. M.; Ahmed, I.; Wahnström, G.; Berastegui, P.; Börjesson, L.; Eriksson, S. G. *Solid State Ionics* **2009**, *180*, 22.
(7) Karmonik, C.; Hemplemann, R.; Cook, J.; Güthoff, F. *Ionics* **1996**, *2*, 69.
(8) Pionke, M.; Mono, T; Schweika, W.; Springer, T.; Schober, H. *Solid State Ionics* **1997**, *97*, 497.
(9) Wilmer, D.; Seydel, T.; Kreuer, K. D. *Mater. Res. Soc. Proc.* **2007**, *972*, 15.
(10) Braun, A.; Duval, S.; Ried, P.; Embs, J.; Juranyi, F.; Strässle, T.; Stimming, U.; Hempelmann, R.; Holtappels, P.; Graule, T. *J. Appl. Electrochem.* **2009**, *39*, 262103.
(11) Mezei F. *Neutron Spin-Echo: Lecture Notes in Physics*; Springer: Heidelberg, 1980; Vol. *28*.
(12) Mezei, F. *Z. Phys.* **1972**, *255*, 146.
(13) Mezei, F.; Pappas, C.; Gutberlet, T. *Neutron Spin Echo Spectroscopy: Basics, Trends and Applications*; Springer: Heidelberg, 2003.
(14) Schober, T.; Bohn, H. G. *Solid State Ionics* **2000**, *127*, 351.

 Published on Web 10/28/2009 

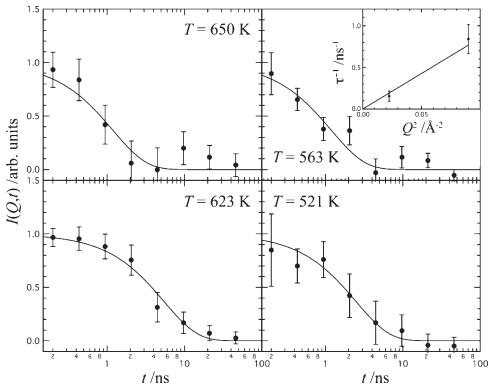


**Figure 1.** $I(Q,t)$ at $T = 650$ ($Q = 0.2$ Å$^{-1}$), 623 ($Q = 0.2$ Å$^{-1}$), 563 ($Q = 0.3$ Å$^{-1}$), and 521 K ($Q = 0.3$ Å$^{-1}$). The solid lines are fits to $I(Q,t) = e^{-t/\tau(Q)}$. Inset in upper right panel: $Q^2$-dependence of the relaxation rate at $T = 563$ K, where the line represents a fit to $\tau^{-1} = DQ^2$.

$\tau^{-1}(Q) = DQ^2$ where $D$ is the self-diffusion coefficient, while a more complex motion would consequently result in a more complex shape of $I(Q,t)$; see further below.[15] Data were obtained for the following temperatures and $Q$-values: 473 K ($Q = 0.3$ Å$^{-1}$), 521 K ($Q = 0.3$ Å$^{-1}$), 563 K ($Q = 0.15$ and 0.3 Å$^{-1}$), 623 K ($Q = 0.2$ Å$^{-1}$), and 650 K ($Q = 0.2$ Å$^{-1}$). Information about the normalization of $I(Q,t)$, following a nonstandard procedure due to a low polarization, is found in the Supporting Information.

Figure 1 shows the normalized $I(Q,t)$, obtained in the experiment at 521−650 K. For all temperatures, $I(Q,t)$ is manifested by a relaxational decay in the time-range 1−5 ns. This decay can be well fitted to a single exponential function, as represented by the solid lines in Figure 1, although it should be noted that a more complicated decay can, at this point, not be ruled out given the limited accuracy of the data. In this context we note that on the measured time- and length-scales oxygen diffusion is negligible at the investigated temperatures,[1] knowing that $Q = 0.15$−$0.3$ Å$^{-1}$ corresponds to a length-scale of ∼20−40 Å in real space. We can therefore safely assign the decay in $I(Q,t)$ to proton dynamics. Furthermore, since neutron scattering on protons is predominantly incoherent, $I(Q,t)$ can, in our case, be approximated with the self-intermediate scattering function; that is, largely only self-dynamics of the protons is measured.

For the temperature 563 K we have determined the relaxation rate ($\tau^{-1}$) for two $Q$-values and as can be seen in the inset in Figure 1 $\tau^{-1}$ follows a $Q^2$-behavior. The fact that the relaxation function in the experiment is well described by a single exponential decay and follows a $Q^2$-behavior points toward that we are observing translational diffusion of the protons.[15] This implies that already on a length-scale of 20 Å, which corresponds to a distance of ∼5 unit cell lengths (the lattice parameter of 10Y:BZO is 4.20 Å),[14] potential local traps or other "imperfections" in the structure that may severe the proton transport have averaged out. Therefore, we have extracted a diffusion coefficient assuming a $\tau^{-1}(Q) = DQ^2$ dependence also for the other temperatures and the result from this analysis is

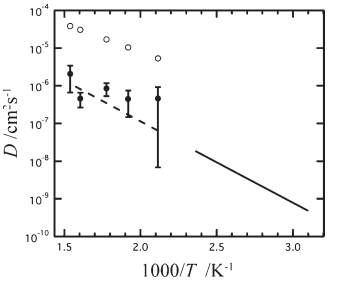


**Figure 2.** Diffusion constant obtained from NSE (●), first-principles calculations (○), and conductivity measurements (line). The dashed line is an extrapolation of the latter result.

shown in the Arrhenius plot in Figure 2. It is evident that the obtained values are consistent between the different temperatures, which provides support that our analysis is physically reasonable. Moreover, these values are in the same range as those obtained from frequency-resolved neutron scattering on the same material, namely $6.8 \times 10^{-7}$ cm$^2$ s$^{-1}$ at 673 K and $5.3 \times 10^{-7}$ cm$^2$ s$^{-1}$ at 573 K, although it should be noted that those measurements were performed at the limit of what the spectrometer could resolve.[9]

To further corroborate our analysis of the NSE data we have also modeled $I(Q,t)$ using a kinetic model based on first-principles calculations as described in the Supporting Information.[16,17] The first-principles calculations were carried out within the framework of density functional theory (DFT); details on the settings can be found in ref. 16 and in the Supporting Information. From the DFT calculations the barriers to proton transfer and hydroxyl rotation in the vicinity of and far from dopants were assessed and used as input parameters for the kinetic model. The calculated diffusion barriers far from Y-dopants are found to be 0.20 and 0.18 eV for the proton transfer and hydroxyl rotation motion, respectively. The binding energy to a Y-dopant is 0.16 eV, and we find that the influence of the Y-dopant on the energetics for the proton is quite extended in space, including both the first and the second coordination shells. For the doping level of 10% it implies that the region influenced by the dopants amounts to about half of the lattice sites. A conventional trapping-diffusion description, where the extension of the traps is ignored, thus cannot be used.

Figure 3 shows the calculated intermediate scattering function, $I_{calc.}(Q,t)$, at $T = 563$ K and for a dopant concentration corresponding to 12.5%. Results are shown for momentum transfers $Q = 0.3$, 0.5, 2.0 Å$^{-1}$ and the long-range diffusion limit $Q \rightarrow 0$, in which the scattering function is given by a single exponential with a characteristic relaxation rate $\tau^{-1}(Q) = DQ^2$, where $D$ is the calculated diffusion coefficient.[15] Since the calculated scattering functions are plotted against $Q^2t$ they will collapse onto a single curve as long as we are in the long-range diffusion regime. As seen in Figure 3, this is

(15) Bée M. *Quasielastic Neutron Scattering*; IOP Publishing: Bristol, 1988.

(16) Björketun, M. E.; Sundell, P. G.; Wahnström, G. *Phys. Rev. B: Condens. Matter* **2007**, *76*, 054307.

(17) Björketun, M. E.; Sundell, P. G.; Wahnström, G.; Engberg, D. *Solid State Ionics* **2005**, *176*, 3035.

clearly the case up to, at least, $Q = 0.5$ Å$^{-1}$; in fact a deviation from the diffusive behavior cannot be seen until $Q = 0.8$ Å$^{-1}$. Thus, for the $Q$-values probed in the NSE experiment we indeed expect to observe the long-range diffusional process. Only for larger $Q$-values does $I_{calc.}(Q,t)$ deviate clearly from the single exponential behavior. For example, at $Q = 2.0$ Å$^{-1}$ in Figure 3 one can observe a more complicated relaxation function. This is indicative of trapping, that is, that the proton spends an extended time in the vicinity of dopant atoms before it diffuses further, thus decreasing the long-range proton mobility. The view of dopant atoms acting as well localized trapping centers has previously been proposed based on quasielastic neutron scattering data,[3] muon spin-relaxation experiments,[18] and computer simulations.[19−21] It should be noted that for lower dopant concentrations the transition from a single exponential to a more complicated relaxation will occur at smaller $Q$-values.

From the kinetic model based on first-principles calculations we have also determined the diffusion constant for five different temperatures. These values are included in Figure 2 together with the values obtained from conductivity measurements[22] of the same material for comparison. The conductivity measurements were performed at lower temperatures than our NSE measurements, but if one extrapolates the conductivity data we find a good agreement between the proton diffusion constants obtained from the two different experimental techniques. The kinetic model on the other hand overestimates the diffusion constant by about 1 order of magnitude. However, the accuracy of the obtained potential energy surface is limited by the accuracy of the approximation for the exchange-correlation functional. It is known that generalized gradient approximations (used in the present study) have a tendency to underestimate energy barriers for proton transfer processes.[23] An underestimation of 0.1 eV, which is not at all unreasonable, would increase the rate by about a factor of 10 at the present temperatures. Changes in the potential energy surface will also influence the value for the vibrational frequencies entering the expression for the prefactors for the individual jumps. Furthermore, our modeling of the prefactors for the individual rates[16] can be improved by incorporating more vibrational degrees of freedom, and the diffusion model we have employed assumes that consecutive proton jumps in the structure are uncorrelated.

One should note that the diffusion constant probed in conductivity measurements reflects the bulk diffusion of protons between grain boundaries, with a length-scale of the order 1 $\mu$m, which is much longer than the length-scale over which the proton diffusion is investigated by NSE, ~20−40 Å in our case. This suggests that there is no new potential feature on a larger length-scale that has not been experienced by the proton on the shorter length-scale probed by NSE. Only for $Q$-values larger than 0.5 Å$^{-1}$, corresponding to distances shorter than ~three unit cell lengths, trapping effects are expected in this material. By extending the $Q$-range to higher $Q$-values in the NSE experiment, it should be possible to observe the crossover from a single exponential at low $Q$, typical for long-range proton diffusion, to a more complex form at larger $Q$-values, suggesting that several processes are reflected in $I(Q,t)$. Such investigations may for example give information about the existence/nature of traps, an often debated subject for hydrated perovskites.

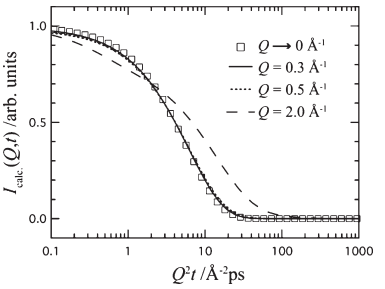


**Figure 3.** Calculated intermediate scattering functions, $I_{calc.}(Q,t)$, for various momentum transfer values, $Q$, at 563 K.

To conclude we present data from the first NSE experiment on a proton-conducting perovskite, namely, hydrated $BaZr_{0.90}Y_{0.10}O_{2.95}$, and demonstrate that NSE can be beneficially applied to investigate the protonic self-diffusion in this class of materials, and most likely also in many other types of solid-state proton conductors, such as proton-conducting polymers,[24] solid acids,[25] and alkali thio-hydroxogermanates.[26] Furthermore, we show that NSE, which indeed is the only neutron scattering technique that gives access to the long time-scales needed to accurately investigate the comparatively slow proton diffusion in hydrated perovskites can be powerfully combined with kinetic modeling based on first-principles calculations, since both techniques cover the same time- and length-scales.

**Acknowledgment.** We are grateful for financial support from the Swedish agencies VR, NFSM, and SSF via the ATOMICS program. Allocation of beam time at ILL and of computer resources through the SNAC are also gratefully acknowledged.

**Supporting Information Available:** Details of the sample preparation, the NSE experiment, and the kinetic modeling based on first-principles calculations (PDF). This material is available free of charge via the Internet at http://pubs.acs.org.

(18) Hempelmann, R.; Soetramo, M.; Hartmann, O.; Wäppling, R. *State Ionics* **1998**, *107*, 269.
(19) Davies, R. A.; Islam, M. S.; Gale, J. D. *Solid State Ionics* **1999**, *126*, 323.
(20) Islam, M. S.; Slater, P. R.; Tolchard, J. R.; Dinges, T. *Dalton Trans.* **2004**, 3061.
(21) Islam, M. S.; Davies, R. A.; Gale, J. D. *Chem. Mater.* **2001**, *13*, 2049.
(22) Kreuer, K. D.; Adams, S.; Münch, W.; Fuchs, A.; Klock, U.; Maier, J. *Solid State Ionics* **2001**, *145*, 295.
(23) Barone, V.; Adamo, C. J. *J. Chem. Phys.* **1996**, *105*, 11007.
(24) Schuster, M. F. H.; Meyer, W. H. *Annu. Rev. Mater. Res.* **2003**, *33*, 233.
(25) Haile, S. M.; Boysen, D. A.; Chisholm, C. R. I.; Merle, R. B. *Nature* **2001**, *410*, 910.
(26) Karlsson, M.; Matic, A.; Panas, I.; Bowron, D. T.; Martin, S. W.; Nelson, C. R.; Martindale, C. A.; Hall, A.; Börjesson, L. *Chem. Mater.* **2008**, *20*, 6014.